The EMBO Journal Vol. 22 No. 21 pp. 5679–5689, 2003

Cytosolic HSP90 associates with and modulates the *Arabidopsis* RPM1 disease resistance protein

David A.Hubert[1], Pablo Tornero[1,2], Youssef Belkhadir[1], Priti Krishna[3], Akira Takahashi[4], Ken Shirasu[4] and Jeffery L.Dangl[1,5,6]

[1]Department of Biology, [5]Curriculum in Genetics and Department of Microbiology and Immunology, Coker Hall, Room 108, CB 3280, University of North Carolina at Chapel Hill, Chapel Hill, NC 27599, USA, [3]Department of Biology, University of Western Ontario, London, ON N6A 5B7, Canada and [4]Sainsbury Laboratory, John Innes Centre, Colney, Norwich NR4 7UH, UK

[2]Present address: IBMCP, Universidad Politecnica de Valencia, Camino de Vera s/n, 46022 Valencia, Spain

[6]Corresponding author
e-mail: dangl@email.unc.edu

D.A.Hubert, P.Tornero and Y.Belkhadir contributed equally to this work

The *Arabidopsis* protein RPM1 activates disease resistance in response to *Pseudomonas syringae* proteins targeted to the inside of the host cell via the bacterial type III delivery system. We demonstrate that specific mutations in the ATP-binding domain of a single *Arabidopsis* cytosolic HSP90 isoform compromise RPM1 function. These mutations do not affect the function of related disease resistance proteins. RPM1 associates with HSP90 in plant cells. The *Arabidopsis* proteins RAR1 and SGT1 are required for the action of many R proteins, and display some structural similarity to HSP90 co-chaperones. Each associates with HSP90 in plant cells. Our data suggest that (i) RPM1 is an HSP90 client protein; and (ii) RAR1 and SGT1 may function independently as HSP90 cofactors. Dynamic interactions among these proteins can regulate RPM1 stability and function, perhaps similarly to the formation and regulation of animal steroid receptor complexes.

Keywords: HSP90/plant disease/RAR1/RPM1/SGT1

Introduction

Our understanding of disease resistance specificity in plants centers on the structure and function of pathogen-specific *R*esistance (*R*) gene products. R proteins confer resistance to pathogen strains expressing a molecule that specifically triggers its action (Dangl and Jones, 2001). The largest class of R protein contains a nucleotide-binding site (NB) and leucine-rich repeats (LRRs), and are termed NB-LRRs (Dangl and Jones, 2001). The repertoire of R proteins, though deployed with broad population polymorphism, may still not be sufficiently diverse to mediate direct recognition of all relevant pathogens. The question of repertoire size, among others, drove the formulation of the 'guard hypothesis'. Here, pathogen molecules that trigger R action are most easily thought of as virulence factors whose presence is sensed by the host cell. Experimental evidence supports this model, though it is not yet fully generalizable (Dangl and Jones, 2001; Holt *et al*., 2003). NB-LRR activation may include a large conformational change, perhaps akin to the 'jackknife model' leading to proximity-induced activation as proposed for Apaf-1 (Moffett *et al*., 2002; Hwang and Williamson, 2003). This, in turn, leads to a series of cellular events that collectively form the defense response (Holt *et al*., 2003). It is unclear what portion of this diverse defense response is actually required to halt pathogen growth.

Arabidopsis RPM1 is an NB-LRR protein that confers recognition to bacterial strains expressing either of two divergent type III effector genes, *avrRpm1* or *avrB* (Grant *et al*., 1995). These two type III effector proteins have virulence function on hosts lacking *RPM1* (*rpm1*; disease susceptible; Ashfield *et al*., 1995; Ritter and Dangl, 1995). Recognition of AvrRpm1 or AvrB by RPM1 may be the consequence of their action on *Arabidopsis* RIN4 (RPM1-interacting protein 4). RIN4 is a protein of unknown function and is phosphorylated in response to the presence of either AvrRpm1 or AvrB (Mackey *et al*., 2002). RIN4 can interact with RPM1, AvrRpm1 and AvrB *in vivo*. All four of these proteins localize to the plasma membrane (Boyes *et al*., 1998; Nimchuk *et al*., 2000; Mackey *et al*., 2002).

A limited set of genetically defined proteins are broadly required for the action of *Arabidopsis R* gene subsets (Dangl and Jones, 2001). The *ndr1* mutation compromises the function of a subset of NB-LRR R proteins (Century *et al*., 1997). NDR1 is a putative glycosylphosphatidylinositol (GPI)-anchored protein (B.Staskawicz, personal communication). Mutations in *RAR1* and *SGT1b*, one of two *SGT1* orthologs in *Arabidopsis*, compromise the function of many R proteins (Azevedo *et al*., 2002; Muskett *et al*., 2002; Tör *et al*., 2002; Tornero *et al*., 2002b). Plant SGT1 proteins share similarity with the yeast SGT1 protein, a regulator of the SCF ubiquitin ligase complexes in a variety of cellular processes (Kitigawa *et al*., 1999). RAR1 and SGT1 can interact *in vivo*, and presumably function together (Azevedo *et al*., 2002).

RPM1 function is compromised by *ndr1* and by *rar1* but, surprisingly, is not compromised by either *sgt1a* or *sgt1b*. Because an *sgt1a*/*sgt1b* double mutant is lethal (A.Takahashi and K.Shirasu, in preparation), overlapping contributions of these genes to *RPM1* function cannot be determined. We performed a large-scale screen for loss of *RPM1*-mediated hypersensitive cell death (hypersensitive response; HR) in response to conditional expression of an *avrRpm1* transgene (Tornero *et al*., 2002a). We describe here four mutant alleles of the *Arabidopsis HSP90.2* gene that caused loss of *RPM1*-specified HR and disease

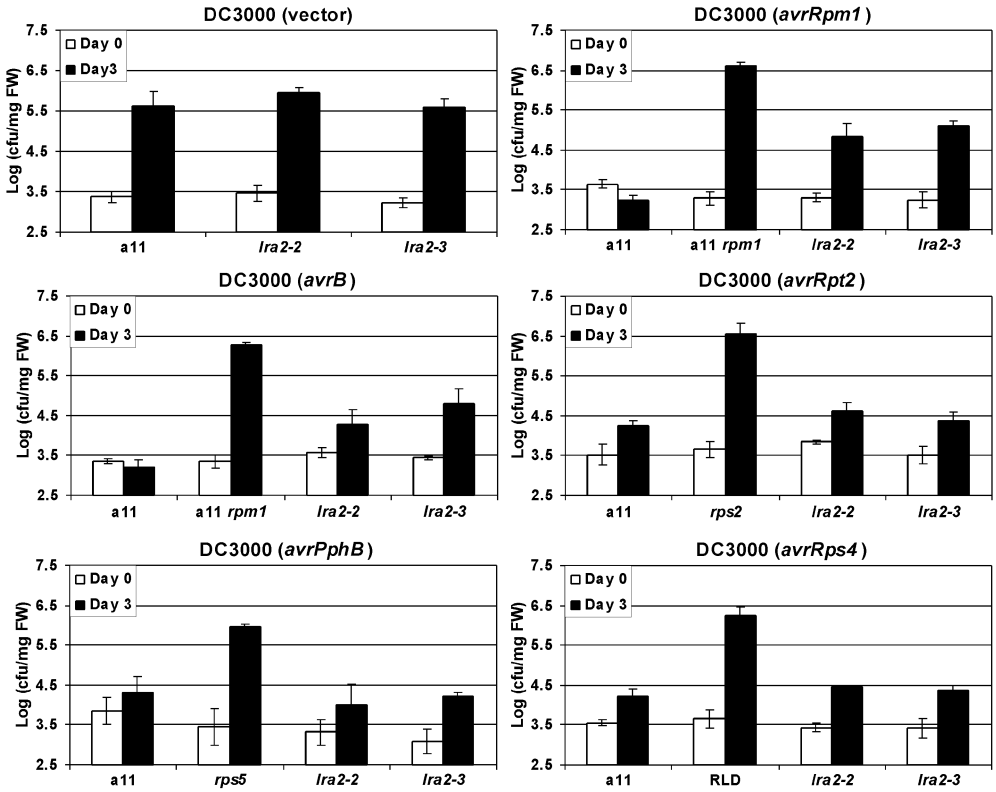

Fig. 1. Mutations in *lra2* specifically affect *RPM1* signaling. Growth of *Pst* DC3000 containing the indicated avirulence genes in *lra2* mutants and corresponding controls (used throughout). The a11 line is the Col-0 parent containing the estradiol-inducible *avrRpm1* transgene (Tornero *et al*., 2002a). The a11;*rpm1-1* line is the a11 transgene crossed into an isogenic *rpm1-1* background. Bacterial numbers here and in Figures 2 and 3 are expressed as the $\log_{10}$ of c.f.u/mg fresh weight (f.w.) (Tornero and Dangl, 2001). Error bars indicate ±SE. Growth of *Pst* DC3000(vector) did not show a significant difference in growth in *lra2* mutants. *Pst* DC3000(*avrRpm1*) and *Pst* DC3000(*avrB*) exhibited consistent increased growth in *lra2* mutants intermediate to growth observed in *rpm1* mutants in four independent experiments.

resistance in that screen. This represents the first phenotype attributed to mutation of a plant cytosolic *HSP90*.

We demonstrate that RPM1 is the first client protein described for plant cytosolic HSP90, using as criteria (i) *in vivo* HSP90–RPM1 interaction; (ii) modulation of RPM1 function by particular mutant alleles of the HSP90.2 isoform; and (iii) greatly decreased steady-state RPM1 levels in these *hsp90.2* mutant backgrounds. We describe genetic interactions between *HSP90.2* and both *RPM1* and *NDR1*. We provide evidence for *in vivo* interactions between HSP90s and both RAR1 and SGT1. Thus, we describe a possible mechanism by which RAR1 and SGT1 affect disease resistance protein signaling through probable cofactor interactions with cytosolic HSP90s.

Results

lra2 mutations specifically affect RPM1-mediated pathogen recognition

We screened ~500 000 ethyl methanesulfonate (EMS)-mutagenized *Arabidopsis* M2 individuals for mutants affecting recognition of *avrRpm1*. Among others, we identified four allelic mutations that we called *lra2-1*, *lra2-2*, *lra2-3* and *lra2-4* (*lra2*; *l*oss of *r*ecognition of a*vrRpm1*; Tornero *et al*., 2002a). Two of these, independently isolated, were later found to carry the same mutation.

Both the *lra2-2* and *lra2-3* alleles have an intermediate effect on *RPM1* function (as did the other two alleles, data not shown) measured by pathogen growth and disease symptoms following challenge with *Pseudomonas syringae* pv *tomato* (*Pst*) strain DC3000 expressing either *avrRpm1* or *avrB* (Figure 1; data not shown). We did not see a significant effect on other *R* genes active against different type III effectors from *P.syringae* (Figure 1). *RPM1*-mediated HR was also altered, but not completely abolished, in the *lra2* mutants in response to infiltration with *Pst* DC3000(*avrRpm1*). This is similar to the effect of *rar1* on *RPM1*-mediated HR (Tornero *et al*., 2002b). While normal *RPM1*-mediated HR occurs 5–8 h after inoculation, we observed a low frequency of HR on leaves from all *lra2* alleles by 20 h (data not shown). The effect of *lra2* mutations on the HR was also specific to RPM1.

Basal resistance against virulent pathogens (*Pst* DC3000) was not significantly affected (Figure 1). We also observed no alteration in the responses of *lra2* alleles to infection with a series of *Peronospora parasitica* isolates (Holub *et al*., 1994). This included isolates that were either specifically recognized by various *R* genes in the *lra2* parental background [Cala2 (recognized by *RPP1a*), Emoy2 (*RPP4*), Emwa1 (*RPP4*) and Hiks1 (*RPP7*)] or caused downy mildew disease (Emco5 and Noco2) (data not shown).

We observed that *lra2-2* and *lra2-4* displayed a partial penetrance phenotype for both HR and onset of disease

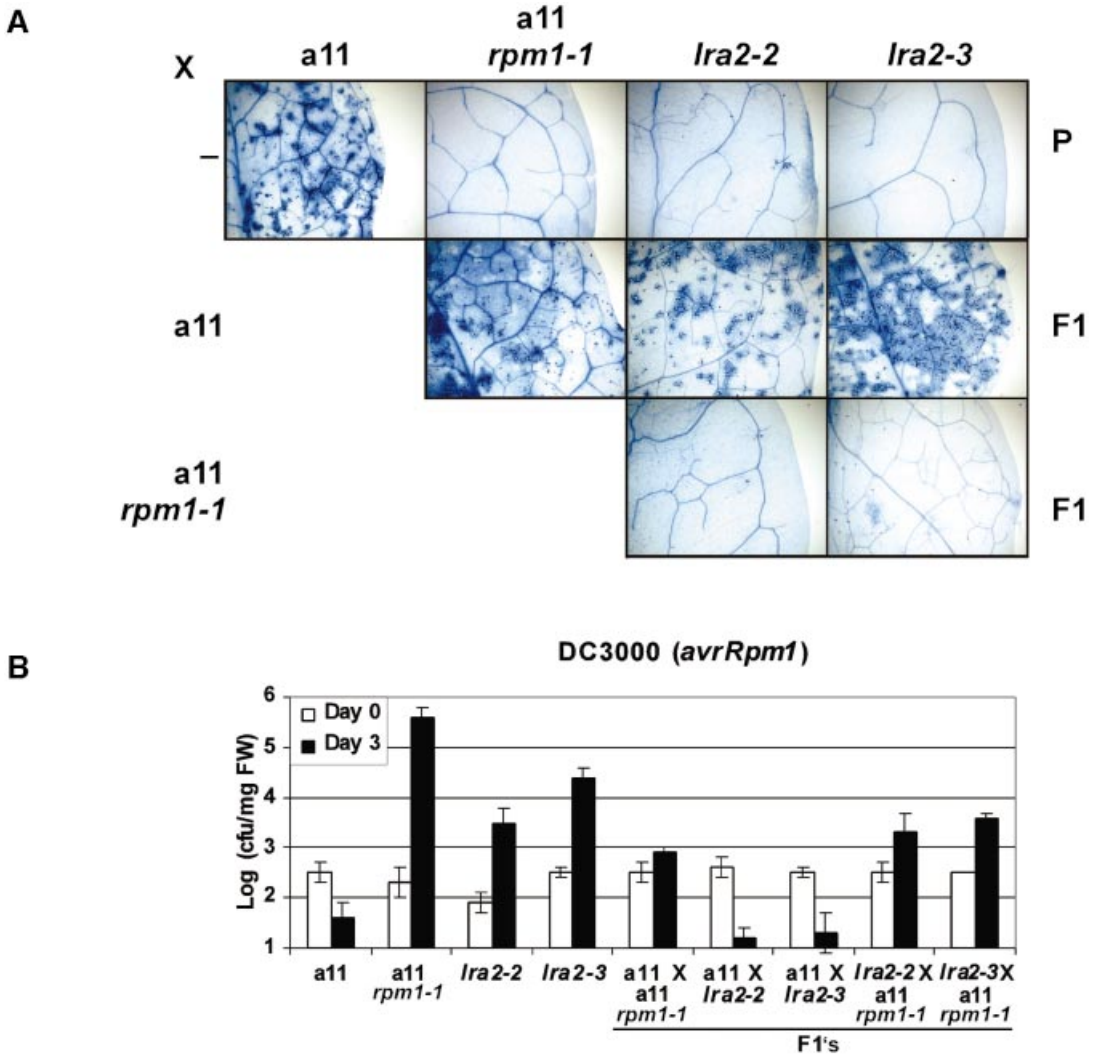

Fig. 2. *LRA2* and *RPM1* interact genetically. (**A**) Trypan blue staining of an HR assay following estradiol induction of *avrRpm1* expression. Two-week-old plants were treated with 10 μM estradiol with 0.02% silwet, and stained with trypan blue 2 days later. Row 1 displays parental responses to conditional expression of *avrRpm1*. Row 2 displays that the *lra2* and *rpm1* mutants are recessive. Row 3 shows that *rpm1*;*lra2* trans-heterozygotes do not express HR. Three independent repetitions were performed. (**B**) Growth of *Pst* DC3000(*avrRpm1*) in the same genotypes as (A). Error bars indicate ±SE of triplicates from this experiment. The experiment was performed six times with similar results.

symptoms. After inoculation with low doses of *Pst* DC3000(*avrRpm1*), *lra2-2* and *lra2-4* plants either developed symptoms characteristic of disease (in 0–80% of plants) or were completely asymptomatic (data not shown). Progeny from self-fertilization of either symptomatic or asymptomatic individuals displayed similar variable penetrance in the next generation (data not shown). The partially penetrant disease phenotype did not influence the standard deviation in our bacterial growth assays (see Figure 1).

LRA2 and RPM1 interact genetically

We made test cross F_1s between *rpm1* and all *lra2* alleles and assayed two phenotypes for allelism: the HR resulting from estradiol induction of the *avrRpm1* transgene contained in these lines (Tornero *et al*., 2002a) and bacterial symptoms resulting from *Pst* DC3000(*avrRpm1*) infection. Both of these assays initially suggested that *lra2* was allelic to *rpm1* in the F_1 generation. However, F_2 progeny from these F_1s contained a large percentage of phenotypically wild-type individuals. This is inconsistent with allelism, and is consistent with non-allelic non-complementation. In this condition, F_1 individuals of a cross between two unlinked recessive mutants (each mutation thus heterozygous) display a phenotype similar to either homozygous single mutant. This often indicates that the two genes act together, that the protein products physically interact or are part of the same protein complex, or that half the wild-type dose of the two, in combination, is insufficient for wild-type function (e.g. Belanger *et al*., 1994; Larkin *et al*., 1999).

We assayed HR response and bacterial growth in the *lra2* alleles and in various F_1 progeny (Figure 2) to address the apparent genetic interaction between *LRA2* and *RPM1*. The wild-type parental plant line, containing the estradiol-inducible *avrRpm1* transgene (called a11; Tornero *et al*., 2002a) responded to estradiol with a strong HR (Figure 2A). The isogenic a11;*rpm1-1* control (Tornero

et al., 2002a) and the tested *lra2* alleles exhibited no HR. The obvious induction of HR in F_1 progeny of backcrosses to a11 demonstrated that both *rpm1* and the tested *lra2* alleles were recessive in this assay. Strikingly, F_1 progeny of (a11;*rpm1-1* × *lra2-2* or × *lra2-3*) did not respond to estradiol (Figure 2A). Furthermore, *lra2-2* and *lra2-3* partially compromised *RPM1* inhibition of bacterial growth, and were fully recessive for this phenotype when assayed as F_1s backcrossed to the a11 parental line (Figure 2B). The F_1 progeny of (a11;*rpm1-1* × *lra2-x*) exhibited modest, but reproducible, reduction of *RPM1* function. These plants allowed bacterial growth between that of the *lra2* parent and the (a11 × a11;*rpm1-1*) F_1 control. This genetic interaction is specific to *lra2* and *rpm1*, as we did not observe non-allelic non-complementation in other trans-heterozygous combinations of mutants affecting the RPM1 pathway tested (tested were *rar1* × *rpm1*, *ndr1* × *rpm1*, *rar1* × *ndr1*, *rar1* × *lra2* and *ndr1* × *lra2*; data not shown). The data in Figure 2 strongly support the conclusion that *rpm1* and *lra2* exhibit non-allelic non-complementation. Our data thus suggest that the respective wild-type RPM1 and LRA2 proteins work in the same pathway, and potentially interact physically.

ndr1 and lra2 display both synergistic and epistatic interactions

Like *lra2*, *ndr1* supported an intermediate level of bacterial growth when challenged with *Pst* DC3000(*avrRpm1*) (Figure 3). Additionally, the *RPM1*-mediated HR is severely attenuated in *lra2* (see above), but not compromised in *ndr1* (Century *et al*., 1995; Tornero *et al*., 2002b). These incomplete phenotypic effects allowed us to assay for genetic interaction between *lra2* and *ndr1*. We constructed *lra2*;*ndr1* double mutants and tested them for bacterial growth and HR. The *lra2*;*ndr1* double mutants were completely compromised for *RPM1* function, allowing as much pathogen growth as an *rpm1* mutant following application of *Pst* DC3000(*avrRpm1*) (Figure 3; note log scale). The *lra2*;*ndr1* double mutant also displayed full loss of *Pst* DC3000(*avrRpm1*)-triggered HR, suggesting that *LRA2* is required for the *RPM1*-dependent HR remaining in *ndr1* mutants. Note that while the *ndr1* allele is a null (Century *et al*., 1997), the *lra2* mutants presented here are not (see below).

LRA2 is HSP90.2

We cloned *LRA2* based on its map position. Our mapping population of disease-susceptible (*lra2;lra2*) individuals narrowed the *LRA2* interval to an ~52 kb region on the bottom arm of chromosome V (see Materials and methods and Supplementary figure 1, available at *The EMBO Journal* Online). We sequenced candidate genes from this interval in the *lra2-1* mutant and found a G/A transition at position 21 937 (nucleotide positions relative to the published sequence of P1 clone MDA7; GenBank accession No. AB011476). This created a G95E mutation in the cytosolic *HSP90.2* (At5g56030; Figure 4A). We sequenced this gene from the other three independently isolated *lra2* alleles and found mutations in *lra2-2* (C21952T; S100F, independently isolated in *lra2-4*) and in *lra2-3* (G21785A; D80N) (Figure 4A). To avoid confusion and to follow accepted nomenclature conventions, we re-designate the *lra2* alleles *hsp90.2-1*, *hsp90.2-2* and *hsp90.2-3* for *lra2-1*, *lra2-2* and *lra2-3*, respectively.

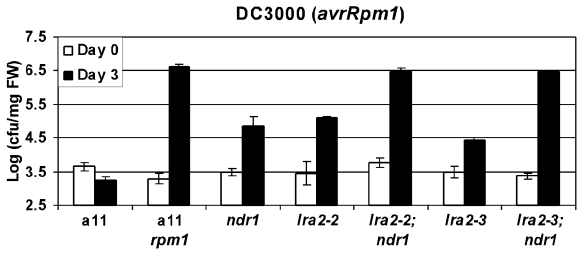

Fig. 3. *lra2* and *ndr1* affect *RPM1* function synergistically. Growth of *Pst* DC3000(*avrRpm1*) in *lra2*;*ndr1* double mutants with corresponding controls, as in Figures 1 and 2. Both *lra2* and *ndr1* single mutants exhibit intermediate growth, while the double mutant exhibits complete susceptibility.

All mutations were within the conserved ATPase domain of this HSP90 (Figure 4A). The *hsp90.2-3* change (D80N; yellow in Figure 4B) alters a residue previously shown to make multiple ATP contacts in the crystal structure of yeast HSP90 (Prodromou *et al*., 1997). The *hsp90.2-1* (G95E) and *hsp90.2-2* (S100F) changes are both adjacent to residues that make direct contact with ATP (N93 and R99). The G95E change should alter the local charge density, while the S100F change results in addition of a large hydrophobic side chain. We used molecular markers based on the mutation to outcross *hsp90.2-3* from the conditional *avrRpm1* expression transgenes (Materials and methods). This line expressed the same significant reduction of RPM1 function as its parent line, measured by both disease symptoms (Figure 5A, compare with Figure 1) and pathogen growth (Figure 5B). Thus, the transgenes carrying the estradiol-inducible *avrRpm1* system have no effect on the mutant phenotype. Finally, an insertion allele, *hsp90.2-5* (a T-DNA insertion at approximately nucleotide 23 453, amino acid position 601 of 699, SiGNAL line SALK_058553; Supplementary figure 1) was viable and exhibited no alteration of *RPM1*-mediated resistance (Figure 5B). We did not detect a truncated form by western blot (data not shown), and assume that this allele is a null. We infer that one of the other three highly homologous cytosolic HSP90s compensates for the loss of HSP90.2 (Borkovich *et al*., 1989). *HSP90.2* is constitutively expressed, especially in flower structures and roots (Yabe *et al*., 1994). We observed only very modest pleiotropic developmental changes in the *hsp90.2* mutants (Queitsch *et al*., 2002) (Supplementary figure 2). Thus, the *hsp90.2* alleles identified in our screen are rare, specific, and not compensated for by other HSP90 isoforms.

HSP90 associates with RPM1 in vivo

An RPM1-myc epitope-tagged protein is a peripheral plasma membrane protein (Boyes *et al*., 1998), and fails to accumulate in *rar1* plants (Tornero *et al*., 2002b). We crossed an RPM1-myc transgene (Boyes *et al*., 1998) into both the fully penetrant *hsp90.2-3* allele and the partially penetrant *hsp90.2-2* allele. Both alleles exhibited greatly decreased RPM1-myc levels compared with wild-type plants (Figure 6A). Curiously, *hsp90.2-2* consistently accumulated less RPM1-myc than *hsp90.2-3*. This suggests that the partial penetrance phenotype of *hsp90.2-2* is not simply correlated to RPM1 levels.

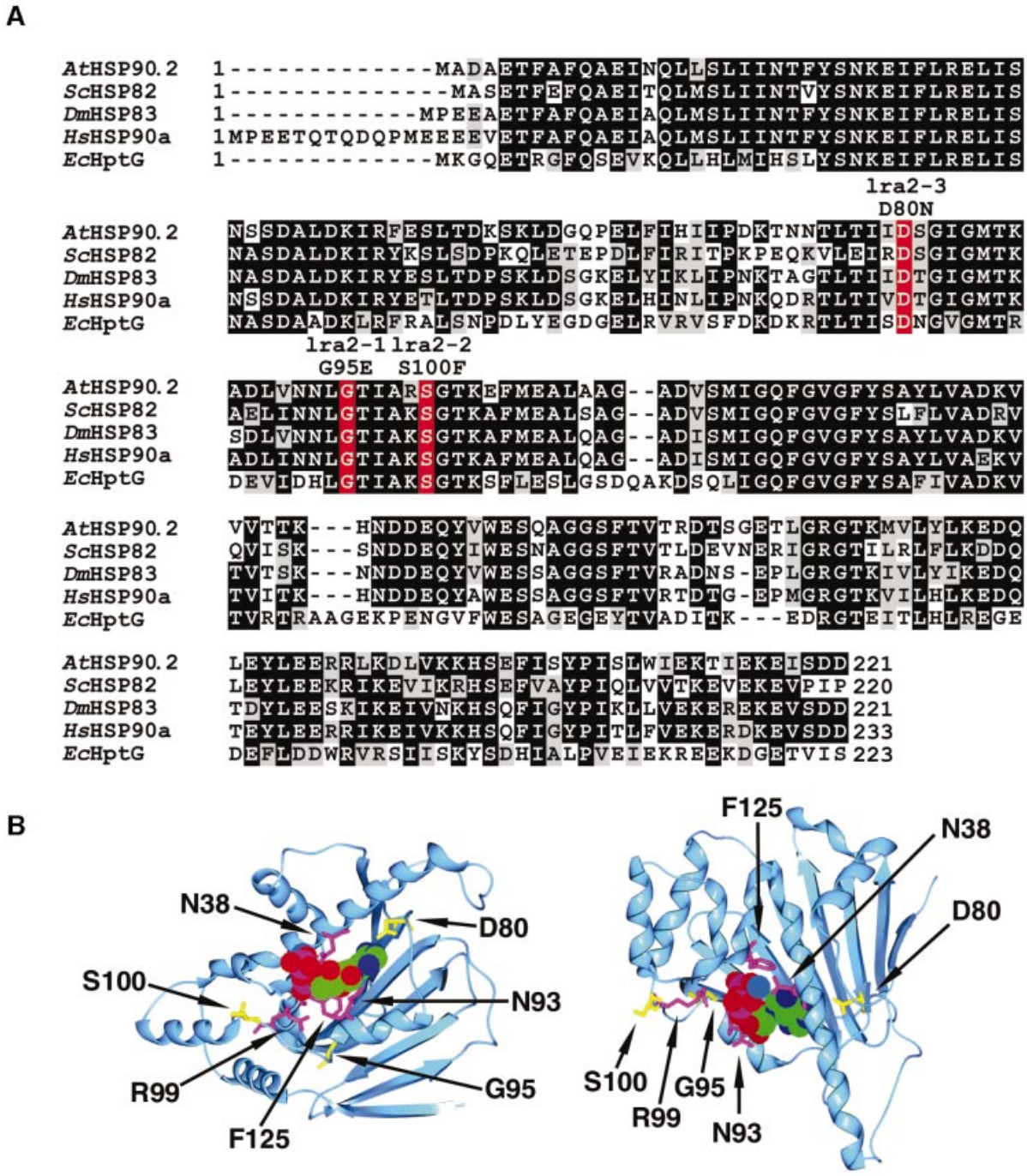

Fig. 4. Clustering of *hsp90.2* mutations in the highly conserved N-terminal ATPase domain. (**A**) Alignment of the N-terminal ATPase domains of HSP90 orthologs across diverse kingdoms, highlighting the residues mutated in our *hsp90.2* alleles in red. Proteins compared: *At*HSP90.2 (swissprot id: HS82_ARATH), *Sc*HSP82 (swissprot id: HS82_YEAST), *Dm*HSP83 (swissprot id: HS83_DROME), *Hs*HSP90a (swissprot id: HS9A_HUMAN) and *Ec*HptG (swissprot id: HTPG_ECOLI). (**B**) Hsp90.2 threaded over the structure of yeast HSP90 bound to ADP (center space filling structure) viewed from two different angles. Residues that make direct interactions with ADP are in violet. The three residues mutated in our *hsp90.*2 alleles are in yellow. Note that D80 makes direct contacts with ADP, and is mutated in *hsp90.*2-*3*.

Given the genetic interaction between *rpm1* and *hsp90.2*, we asked whether HSP90s could co-immunoprecipitate (co-IP) with RPM1-myc. We probed protein blots of anti-myc IPs with an antibody raised against cytosolic HSP90 from *Pharbitis nil*, which should detect all four isoforms of cytosolic HSP90 in *Arabidopsis* (Krishna *et al*., 1997). We successfully detected HSP90 in IPs from *RPM1-myc* plant extracts, but not in IPs from *rpm1* mutant extracts (Figure 6B). The HSP90 antibody failed to detect a clear difference in protein levels between our point mutants or insertion allele and wild-type (data not shown). We therefore cannot ascertain whether the HSP90 detected in our co-IPs is, or contains, HSP90.2. We were unable to detect HSP90 in anti-RIN4 co-IPs, but could co-IP RPM1-myc with anti-RIN4 from the same extracts (data not shown). These data suggest that RIN4 and HSP90 interactions with RPM1 might be mutually exclusive.

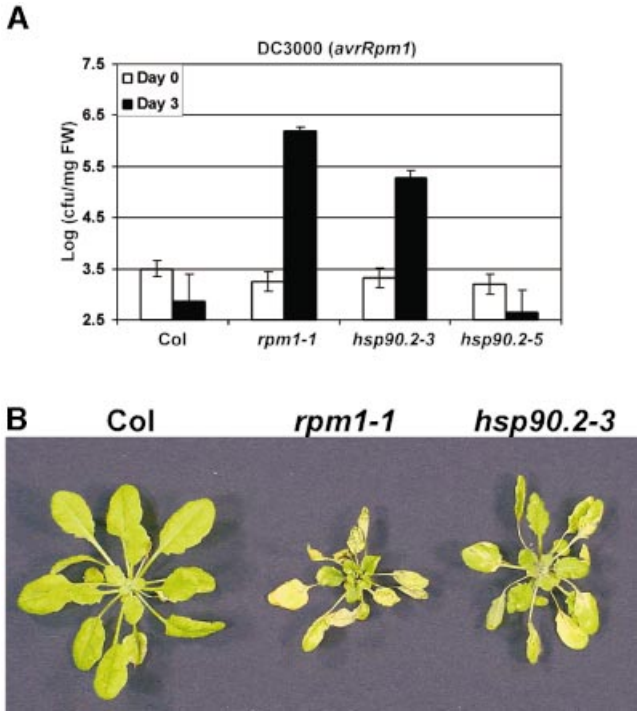

Fig. 5. *RPM1* function is not compromised by an *hsp90.2* insertion allele, and the *hsp90.2-3* phenotype is independent of the conditional *avrRpm1* expression system. (**A**) Bacterial growth assay with *Pst* DC3000(*avrRpm1*). The *hsp90.2-5* (Salk 058553) T-DNA insertion allele displays a wild-type response to *Pst* DC3000(*avrRpm1*). (**B**) In contrast, the *hsp90.2-3* allele outcrossed from the transgenic, conditional *avrRpm1* expression system is still compromised for *RPM1* function. This line, and controls, were spray infected with *Pst* DC3000(*avrRpm1*), and still exhibit symptoms intermediate to a full loss-of-function *rpm1* mutant.

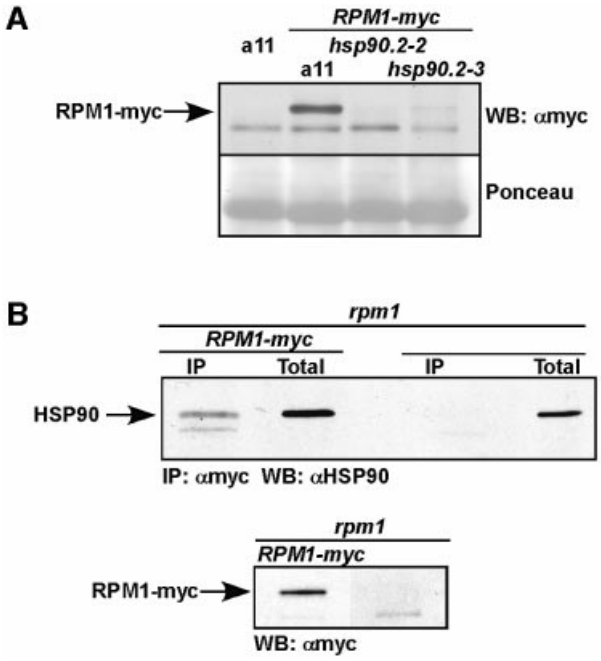

Fig. 6. HSP90 interacts with RPM1. (**A**) *hsp90.2* mutations severely affect RPM1-myc accumulation. A 40 μg aliquot of total protein was loaded and western blots were probed with anti-myc monoclonal antibody. (**B**) Top: anti-myc and co-IPs demonstrate that HSP90 associates with RPM1-myc in planta. The relative amounts of protein from the immune pellet and the total extracts are not equivalent. The pellet is over-represented by 20-fold. This experiment is representative of six independent replicates for RPM1-myc. Bottom: control showing specificity of IP reagents, and that RPM1-myc is extracted from transgenic lines in appropriate mutant backgrounds under the conditions used for the co-IP.

Disease signaling components RAR1 and SGT1 also associate with HSP90 in planta

RAR1 and SGT1 can be co-immunoprecipitated from plant cell extracts (Azevedo *et al*., 2002). There are also structural similarities between plant SGT1 and animal proteins required for HSP90 assembly and function (Dubacq *et al*., 2002; Garcia-Ranea *et al*., 2002; see Discussion). These observations prompted us to explore the physical relationships between RAR1, SGT1 and HSP90.

We used antibodies raised against either RAR1 or SGT1 (Azevedo *et al*., 2002) to IP HSP90 from total plant extracts. We found that anti-RAR1 is able to co-IP HSP90 from wild-type extracts, but not from *rar1-20* extracts (Figure 7A). *Arabidopsis* contains two *SGT1* genes encoding proteins of slightly different mobility (Austin *et al*., 2002; Tör *et al*., 2002); both are detected by our antisera under the IP conditions used. We found that anti-SGT1 antibody is consistently able to co-IP HSP90 from wild-type Col-0 and Ws-0 extracts (six out of six experiments; Figure 7B). However, we detected no, or only very low amounts, of HSP90 in anti-SGT1 IPs from *sgt1b* extracts in multiple experiments (Figure 7B). This suggests that the majority of HSP90 we detected is associated with SGT1b, and that SGT1a may weakly associate with HSP90. We invariably detected HSP90 in IPs from *sgt1a* extracts (Figure 7B), strengthening this conclusion. Thus, in our experimental conditions, there is a preference for HSP90 to associate with SGT1b compared with SGT1a, consistent with yeast two-hybrid data (A.Takahashi and K.Shirasu, unpublished).

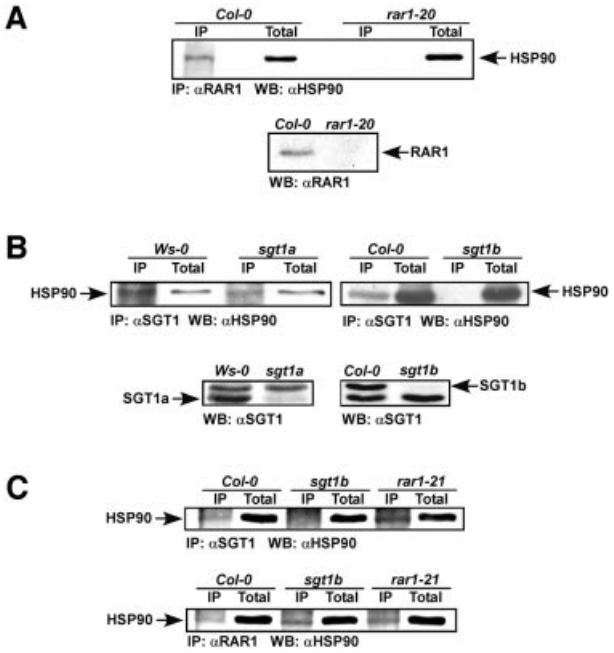

Fig. 7. HSP90 associates with RAR1 and SGT1. (**A**) Hsp90 associates with RAR1 *in planta* (top). The relative amounts of protein from the co-IP pellet and the total extracts are not equivalent. The pellet is over-represented by 10-fold. This experiment is representative of two independent replicates. An extraction control is displayed below the co-IP. (**B**) HSP90 displays an apparent preference for SGT1b over SGT1a. (**C**) HSP90 interacts with RAR1 and SGT1b independently. The N-terminal portion of RAR1 containing the CHORD I domain is sufficient for interaction with HSP90. The relative amounts of protein from the co-IP pellet and the total extracts are not equivalent. The pellet is over-represented by 10-fold. This experiment is representative of three out of seven independent replicates for *sgt1b* and four out of four independent replicates for *sgt1a*. Extraction controls beneath the co-IPs demonstrate the differential mobilities of SGT1a and SGT1b and the effect of the respective mutations.

Additionally, we detected HSP90 in anti-SGT1 IPs from *rar1* mutant extracts and in anti-RAR1 co-IPs from *sgt1b* mutant extracts (Figure 7C). This suggests that RAR1 and SGT1b can associate independently with HSP90. We corroborated this finding in the converse experiment (IP with anti-RAR1 and blot with anti-HSP90) using the null *rar1-20* allele (data not shown). We were, surprisingly, able to detect consistently HSP90 from anti-RAR1 IPs in *rar1-21* mutant extracts (Figure 7C). The *rar1-21* mutation introduces a stop codon near the end of the CHORD I domain (Tornero *et al*., 2002b), and consequently lacks the CHORD II domain, known to be the RAR1–SGT1 interaction platform (Azevedo *et al*., 2002). While we were unable to detect this small RAR1 fragment by direct immunoblot, it appears sufficient to IP HSP90, consistent with two-hybrid interaction data presented elsewhere (Takahashi *et al*., 2003).

Artifactual detection of HSP90 in immunoblots is a concern, because it can represent up to 1–2% of total cellular protein (Lai *et al*., 1984). We therefore used several different antisera to test this, and found that none of them could co-IP HSP90 (see Materials and methods), thus suggesting strongly that our data represent specific interactions.

Discussion

We provide genetic and biochemical data demonstrating that RPM1 is a cytosolic HSP90 client. We demonstrate that mutations in the *Arabidopsis HSP90.2* can specifically modulate RPM1 function. RPM1 accumulation is greatly diminished in specific *hsp90.2* missense mutants. We provide pairwise co-IP data demonstrating interactions between HSP90s and RPM1, RAR1 and SGT1. We show that the HSP90 interaction with RAR1 does not require SGT1, nor does the HSP90 interaction with SGT1 require RAR1. Surprisingly, we did not find an association of HSP90s with RIN4, a protein clearly implicated in RPM1 and RPS2 function (Axtell and Staskawicz, 2003; Mackey *et al*., 2003), suggesting that RIN4 and HSP90 association with RPM1-myc might be mutually exclusive.

Our data suggest that RAR1, SGT1 and HSP90 may work together to coordinate RPM1 function. The key questions emerging from our work are: why do specific *hsp90.2* missense mutations result in diminution of RPM1 levels, and hence RPM1 function? Is the requirement for HSP90 in RPM1 signaling indicative of a common regulatory mechanism among the NB-LRR class of R proteins? Do RAR1 and SGT1 act as cofactors for HSP90 in R protein signaling?

Genetic interactions support a quantitative function for HSP90.2 in R-mediated disease resistance

Our four *hsp90.2* missense alleles are recessive and significantly reduce, but do not eliminate, *RPM1* function. They do not reproducibly affect any of the seven other *R* functions tested. The *hsp90.2* alleles exhibit non-allelic non-complementation with *rpm1*, suggesting that the two wild-type proteins act together. The fact that far less steady-state RPM1-myc protein accumulates in two *hsp90.2* alleles provides a simple, dosage-based mechanistic explanation for this genetic observation.

Our results suggest that specific HSP90.2 missense mutations alter RPM1 function. The four *hsp90.2* alleles reported here compare with 95 *rpm1* alleles also identified in this screen (Tornero *et al*., 2002a). RPM1 is 926 amino acids long, HSP90.2 is 699; thus target size cannot explain this mutant ratio. Furthermore, the insertional *hsp90.2-5* allele is viable, apparently null, and exhibited full RPM1 function. We assume that one of the other three cytosolic HSP90s can compensate for the full loss of HSP90.2, as observed in other systems (Borkovich *et al*., 1989). Thus, our *hsp90.2* alleles also prohibit functional compensation. Significantly, we did not recover alleles in any of the other *HSP90* genes as loss of *RPM1* function mutants. Thus, our *hsp90.2* mutants are rare, and suggest a preferential utilization of HSP90.2 in RPM1 accumulation and, hence, in RPM1 function.

Importantly, a mutation exactly orthologous to *hsp90-2.3* (D80N) has been studied in yeast HSP90 (D79N). This mutant yeast protein homodimerizes properly, and a wild-type–mutant mixed dimer exhibits wild-type levels of ATP hydrolysis (Richter *et al*., 2001). However, mutant dimers are unable to bind or hydrolyze ATP (Obermann *et al*., 1998; Panaretou *et al*., 1998), and in competition assays are unable to interfere with ATP hydrolysis, even in 8-fold excess (Richter *et al*., 2001). Interestingly, a

transcriptionally inducible yeast *hsp90* (D79N) also prevented phenotypic compensation by a wild-type, constitutively expressed isoform (Panaretou *et al*., 1998). This may explain how we identified our mutants in plants that normally contain four copies of cytosolic HSP90, as well as suggesting that HSP90 isoforms might have non-overlapping functions in *Arabidopsis*.

Our other two mutations, *hsp90.2-1* (G95E) and *hsp90.2-2* (S100F), have not been identified in screens in other systems. Both are solvent exposed and adjacent to ATP-interacting residues. It is possible that these mutations also interfere with ATP binding. Altered ATP binding/hydrolysis can also directly affect client protein binding and release by HSP90, as well as the interaction of HSP90 with its co-chaperones, thus de-stabilizing the complex (Obermann *et al*., 1998; Panaretou *et al*., 1998).

Our evidence of both synergism (in pathogen growth assays) and epistasis (in an HR assay) between *hsp90.2* and *ndr1* suggests that HSP90 and NDR1 act together in the RPM1-dependent disease resistance response. A requirement for HSP90.2 early in RPM1 signaling is consistent with our proposal that it is part of, or required for the assembly of, a poised RPM1 receptor complex. These results suggest an interesting parallel with animal innate immunity. NDR1 is a putative GPI-anchored protein. In animal systems, HSP90 co-localizes with the GPI-anchored protein CD14, and both act in the TLR4-dependent innate immune response to lipopolysaccharide (Triantafilou *et al*., 2002). Also, HSP90 inhibitors prevent the innate immune response activation by bacterial DNA (Zhu and Pisetsky, 2001). We propose that NDR1 and HSP90 function together, perhaps transiently, during RPM1 signaling.

Could RAR1 and SGT1 function as HSP90 cofactors in disease resistance pathways?

Several observations indicate that RAR1 and HSP90 function together in RPM1-dependent HR. We demonstrated that RAR1 and SGT1 can associate with HSP90 *in vivo*. We noted a severe attenuation of RPM1-dependent HR in *hsp90.2* mutants and we found decreased RPM1-myc stability in *hsp90.2* mutants, two phenotypes observed in *rar1* plants (Tornero *et al*., 2002b). The epistasis of *hsp90.2* over *ndr1* with respect to HR was also observed with *rar1*;*ndr1* double mutants assayed for *RPM1* function, and for the synergistic interaction of *rar1* and *ndr1* in *RPP7*-mediated resistance (Tornero *et al*., 2002b). These data are, in sum, consistent with RAR1 and HSP90 acting together in both RPM1-dependent HR and, possibly more broadly, in NB-LRR function. Our data are further consistent with recent findings demonstrating that RAR1 and NDR1 contribute quantitatively to the function of various NB-LRR R proteins (Muskett *et al*., 2002; Tornero *et al*., 2002b).

Because an *sgt1a*;*sgt1b* double mutant is lethal in *Arabidopsis* (A.Takahashi and K.Shirasu in preparation), it is impossible to determine if SGT1 isoforms have overlapping function in RPM1 signaling. Recent gene silencing experiments corroborate a role for HSP90 in the function of several *R* genes that also require *SGT1* and *RAR1* for their function (Lu *et al.*, 2003). Structural modeling also supports the contention that RAR1 and SGT1 might act as cofactors of HSP90 (Shirasu and Schulze-Lefert, 2003). SGT1 and RAR1 homologs in animals have predicted structural homology to the HSP90 partner protein, p23 (Dubacq *et al*., 2002; Garcia-Ranea *et al*., 2002; see Supplementary figure 3). Additionally, the TPR domain of SGT1 shares structural homology with other HSP90 partner proteins including HOP/STI1 (Garcia-Ranea *et al*., 2002).

We propose that RAR1 and HSP90 normally not only act to maintain RPM1 in a signal competent conformation, but also stabilize RPM1 against degradation. This is reminiscent of the assembly of activation-competent steroid receptors with an HSP90 isoform homodimer and various co-chaperones (Pratt and Toft, 2003). HSP90 binding to the steroid receptor is not sufficient to render the receptor competent; cofactor binding and continual ATP turnover are required to maintain the steroid-binding cleft in a receptive conformation (Pratt and Toft, 2003). Further conformational change accompanies ligand binding.

Inhibition of ATP binding and/or turnover in our *hsp90.2* mutants should result in a locked HSP90 conformation, bound to RPM1 but unable to hold it appropriately, thus leading to RPM1 disappearance. This would mimic the effect on client proteins observed after treatment with the ATP-binding inhibitor geldanamycin in other systems. RPM1 instability is consistent with results showing that HSP90 can rapidly shut off transcriptional responses by binding transcription factors and causing their degradation (Freeman and Yamamoto, 2002). Steroid receptor levels, like RPM1 (Boyes *et al*., 1998), drop after signaling (Lange *et al*., 2000; Wallace and Cidlowski, 2001).

Evidence for a second HSP90 function in protein stability is also emerging. First, human SKP2, a member of the SCF complex, is able to co-immunoprecipitate HSP90b in mouse NIH-3T3 cells (Lyapina *et al*., 1998). Degradation of HSP90 client proteins, triggered by either geldanamycin treatment or overexpression of the E3 ligase CHIP, can be inhibited by the addition of proteasome inhibitors (Whitesell and Cook, 1996; Segnitz and Gehring, 1997; Connell *et al*., 2001). However, full steroid binding is not recovered in these experiments, also suggesting two functions for HSP90. One, reversible by lactacystin, is required for degradation, and another, not completely reversed by lactacystin, is required to mold a steroid-binding complex. Initiation of RPM1 function leads to RPM1 degradation (Boyes *et al*., 1998), perhaps involving SGT1 that is first recruited to an HSP90–RPM1 complex and then guides RPM1 to the proteasome. RAR1 may normally block this conversion, perhaps in conjunction with (or antagonistically to) SGT1. This notion is consistent with our findings that RAR and SGT1 do not require each other to associate with HSP90.

A model where HSP90, in association with RAR1 and SGT1, controls levels of properly poised R protein complexes is consistent with the two functions of HSP90 discussed above—conformational molding and trafficking to the proteasome. Because of both R protein sequence polymorphism and the possibility that R proteins might associate with additional cellular proteins, one could expect differential functional requirements for maintenance of this poised complex. For example, we also could co-IP HSP90 with anti-hemagglutinin (HA) monoclonal antibody detecting an RPS2-HA fusion (data not shown),

suggesting that at least one other NB-LRR protein can interact with a cytosolic HSP90. However, we observed no change in RPS2 function in our mutants. This model is consistent with the fact that RPM1-mediated HR is very fast compared with others, including RPS2, and that RPM1 is degraded following triggering, unlike RPS2 (Axtell and Staskawicz, 2003). A requirement for a finely tuned conformational poise in NB-LRR R protein function was suggested recently using split Rx molecules (Moffett *et al*., 2002).

We thus favor an overall model whereby different NB-LRR R proteins, perhaps in association with the cellular proteins they guard, are kept in active sentinel mode by varying degrees of dynamic re-shaping and maintenance of appropriate steady-state levels driven by HSP90, RAR1 and SGT1. This model can encompass a continuous quantitative function for HSP90 in both the assembly of conformationally charged R protein complexes and the regulation of signal flux through those complexes.

Materials and methods

Plant lines

Transgenic *Arabidopsis* ecotype Columbia (Col-0) (line a11) and *rpm1-1* (line a11r) containing estradiol-inducible *avrRpm1* have been described in Tornero *et al*. (2002a). Mutant lines used (all in Col-0 unless noted) were *ndr1-1* (Century *et al*., 1997), *rar1-20*; a null allele, originally *pbs2* (Warren *et al*., 1999), *rar1-21* (Tornero *et al*., 2002b), *rps2-101C* (Mindrinos *et al*., 1994), *rps5-2* (Warren *et al*., 1998), ecotype RLD (Hinsch and Staskawicz, 1996) as an *rps4* mutant control, *sgt1a* (T-DNA insertion in Ws-0 ecotype; A.Takahashi and K.Shirasu, in preparation), and *sgt1b* (*edm1-1*; Tör *et al*., 2002). We constructed double mutants of *hsp90.2* and *rpm1-1* by identifying F_2 individuals susceptible to *Pst* DC3000(*avrRpm1*) which were molecularly heterozygous for *rpm1-1*, yet did not give rise to resistant offspring in the next generation. The F_3s from such a line were then selected for a homozygous *rpm1-1* mutant. These lines were confirmed after identification of the *hsp90.2* mutations using PCR-based markers. A similar procedure was used for creation of *hsp90.2* and *ndr1* double mutants. A homozygous insertion in the SALK tDNA insertion line 058553 was identified by molecular analysis of a segregating pool. The insertion site was confirmed by sequencing of T-DNA-specific product. Primer sequences for selection of mutations are available on request.

Bacterial strains, inoculation and growth quantification

Pst DC3000 derivatives containing pVSP61 (empty vector), *avrRpm1*, *avrB*, *avrRpt2*, *avrPphB* or *avrRps4* were maintained as described (Ritter and Dangl, 1996). Plant inoculations and counting of the bacteria were performed as described (Tornero and Dangl, 2001). Where indicated, high concentrations of bacteria (OD_{600} = 0.075, 3.75 × 10^7 c.f.u./ml) were infiltrated into the bottom part of the leaf with a blunt syringe to test for the induction of HR.

Estradiol induction

Two-week-old plants grown under short day (8 h) conditions were sprayed with 0.02% silwet L-77 (CKWitco Corporation) and 10 μM β-estradiol (Sigma E 8875) in distilled water from a 10 mM β-estradiol stock dissolved in 100% ethanol (Tornero *et al*., 2002a).

Mapping and tests for disease symptoms

Rough mapping was performed by crossing *hsp90.2* mutants and Landsberg *erecta* (La-*er*). F_2s were tested for *lra2*-like disease symptoms. One- to three-week-old F_2 plants were sprayed with a 10 mM $MgCl_2$ suspension containing *Pst*DC3000(*avrRpm1*) at a concentration of OD_{600} = 0.1 (5 × 10^7 c.f.u./ml) with 0.02% silwet L-77, covered with a clear lid for 4 h, and assessed for chlorosis and other symptoms of *P.syringae* infection 4–6 days later under short day conditions. χ^2 analyses showed that all mutations were recessive: *lra2-1*: 480 wt, 612 mutant χ^2 = 3.843; P = 0.05; *lra2-2*: 217 wt, 89 mutant χ^2 = 2.723, P = 0.099; *lra2-3*: 457 wt, 155 mutant χ^2 = 0.035, P = 0.85. Susceptible F_2 individuals were allowed to self and were confirmed in the F_3 generation. DNA (Ausubel *et al*., 1987) from 41 of these individuals was used in PCR amplification of known PCR-based molecular markers (www.arabidopsis.org) to obtain approximate mapping positions. This interval was refined using molecular markers we developed (available upon request). We used DNA from 939 susceptible F_2 individuals to define a 52 kb interval on P1 clone MDA7. The ~52 kb *LRA2* interval lies between a T/A polymorphism at position 551 (Jander *et al*., 2002) and the published CAPS marker MDA7 (www.arabidopsis.org) at position 52 632 (C/A) relative to the published sequence for P1 clone MDA7 (Kaneko *et al*., 1998). Independent mapping of the *lra2-2* (195 susceptible individuals) and *lra2-3* (312 susceptible individuals) alleles showed similar linkage. All mutations where confirmed by sequencing of both DNA strands.

Alignments and threading analysis

Protein alignments of HSP90 N-termini were made using Align X [a component of Vector NTI Suite 7.1; Informax, Inc. (Frederick, MD)]. This program uses CLUSTALW to make alignments. Parameters used were: gap opening penalty = 10, gap extension penalty = 0.05, gap separation penalty range = 8, percentage identity for alignment delay = 40, and hydrophobic residue gap = GPSNQEKR.

The sequences of AtSGT1a and AtSGT1b were submitted to the threading Meta server [META] (http://bioinfo.pl/meta/) to identify structural templates for homology modeling. The meta server accessed the following fold recognition servers and reported the consensus: bioinbgu [BIOINBGU], 3D-PSSM [3D-PSSM], GenTHREADER [GENTHREADER], FUGUE [FUGUE] and Sam-T99 [SAMT99]. The meta server identified the crystal structure of the TPR1 domain of Hop (PDB ID 1elw) as a structural template for residues 1–115 of AtSGT1a, and the crystal structure of the human co-chaperone P23 (PDB ID 1ejf) as a structural template for residues 156–237 of AtSGT1a. Models of the P23 and TPR domains were built using the Modeler module of the InsightII molecular modeling system from Accelrys Inc. (www.accelrys.com). Figures were created with SPOCK.

Protein blots and co-immunoprecipitations

For detection of RPM1-myc in *hsp90.2-2* and *hsp90.2-3*, we introgressed these mutants into plants expressing *RPM1-myc* from the native *RPM1* promoter (Boyes *et al*., 1998) as described in Tornero *et al*. (2002b). Total protein was extracted in 50 mM Tris–HCl pH 8.0, 1% SDS, 1 mM EDTA, 1 mM 2-mercaptoethanol and 1× plant protease inhibitor cocktail (Sigma). For immunodetection, 40 μg protein samples were electrophoresed on 8% SDS–polyacrylamide gels. Western blots were performed using standard methods and detected with ECL^+ (Amersham).

For co-immunoprecipitations, tissue was first ground in liquid nitrogen with a mortar and pestle. This material was then homogenized by alternate rounds of Polytron (Kinematica) and glass douncer (Kontes Glass Company) in 2 ml of sterile buffer 20 mM Tris–HCl pH 8.0, 0.33 M sucrose,10 mM EDTA, 5 mM dithiothreitol (DTT) and 1× plant protease inhibitor cocktail (Sigma) per 1 g of tissue. Debris was removed by centrifugation at 5000 *g* for 40 min at 4°C. A 1.5 ml aliquot of this supernatant was first pre-cleared by adding 50 μl of protein G–agarose (Boehringer Mannheim) and incubated at 4°C for 60 min on an orbital shaker. The cleared supernatant was then removed and combined with one of the following: 5 μl of the anti-RAR1 (Muskett *et al*., 2002) antibody, 5 μl of anti-SGT1 (Azevedo *et al*., 2002) antibody, 30 μl of a re-suspended anti-HA Affinity Matrix (3F10, Roche) or 30 μl of a re-suspended anti-c-Myc agarose (9E10, Santa Cruz Biotechnology). This was followed by incubation at 4°C for 2 h. A 50 μl aliquot of protein G–agarose was then added to the reactions containing the anti-RAR1 and anti-SGT1 antibodies. All reactions were then rolled at 4°C overnight. Beads were pelleted at 1000 *g* for 5 min. This was followed by four washes in 1.5 ml of 50 mM HEPES pH 7.4, 100 mM NaCl, and 10 mM EDTA pH 8.0. Bound proteins were eluted with 50 μl of sample buffer and run on an 8% polyacrylamide gel, and probed with a polyclonal antibody raised against the C-terminal portion of *P.nil* HSP90 (Krishna *et al*., 1997).

HSP90 was not detected in control immunoprecipitations with four different antibodies, three of which do immunoprecipitate HSP90 via RPM1-myc, RAR1 or SGT1b. Thus, HSP90 is not non-specifically sticking to protein A/G–agarose beads or other matrix reagents. Furthermore, we used antibodies to actin (soluble), ascorbate peroxidase (soluble), BiP (soluble and endoplasmic reticulum), toposiomerase II (nuclear), RD28 (intergral plasma membrane) (Daniels *et al*., 1994) and Tip (tonoplast intrinsic protein). None of these co-immunoprecipitated

HSP90. The absence of HSP90 in these IPs (data not shown) argues for the specificity of our co-IP data.

Supplementary data

Supplementary data are available at *The EMBO Journal* Online.

Acknowledgements

We thank members of the Dangl lab, especially Drs Ben Holt and Gopal Subramaniam, for technical advice, helpful suggestions and critical reading of the manuscript, and Dr Brenda Temple of the UNC-CH Center for Structural Biology for assistance with threading analyses. This work was funded by the NSF-2010 Arabidopsis Project grant IBN-0114795 to J.L.D. P.K. was supported by a research grant from the Natural Sciences and Engineering Research Council of Canada. A.T. and K.S. were supported by BBSRC and Gatsby Charitable Organization.

References

Ashfield,T., Keen,N.T., Buzzell,R.I. and Innes,R.W. (1995) Soybean resistance genes specific for different *Pseudomonas syringae* avirulence genes are allelic, or closely linked, at the *RPG1* locus. *Genetics*, **141**, 1597–1604.

Austin,M.J., Muskett,P.J., Kahn,K., Feys,B.J., Jones,J.D.G. and Parker,J.E. (2002) Regulatory role of *SGT1* in early *R*-mediated plant defenses. *Science*, **295**, 2077–2080.

Ausubel,F.M., Brent,R., Kingston,R.E., Moore,D.D., Seidman,J.G., Smith,J.A. and Struhl,K. (1987) *Current Protocols in Molecular Biology*. J.Wiley and Sons, New York, NY.

Axtell,M.J. and Staskawicz,B.J. (2003) Initiation of *RPS2*-specified disease resistance in *Arabidopsis* is coupled to the AvrRpt2-directed elimination of RIN4. *Cell*, **112**, 369–377.

Azevedo,C., Sadanandom,A., Kitigawa,K., Freialdenhoven,A., Shirasu,K. and Schulze-Lefert,P. (2002) The RAR1 interactor SGT1 is an essential component of *R*-gene triggered disease resistance. *Science*, **295**, 2073–2076.

Belanger,K.D., Kenna,M.A., Wei,S. and Davis,L.I. (1994) Genetic and physical interactions between Srp1p and nuclear pore complex proteins Nup1p and Nup2p. *J. Cell Biol.*, **126**, 619–630.

Borkovich,K.A., Farrelly,F.W., Finkelstein,D.B., Taulien,J. and Lindquist,S. (1989) hsp82 is an essential protein that is required in higher concentrations for growth of cells at higher temperatures. *Mol. Cell. Biol.*, **9**, 3919–3930.

Boyes,D.C., Nam,J. and Dangl,J.L. (1998) The *Arabidopsis thaliana RPM1* disease resistance gene product is a peripheral plasma membrane protein that is degraded coincident with the hypersensitive response. *Proc. Natl Acad. Sci. USA*, **95**, 15849–15854.

Century,K.S., Holub,E.B. and Staskawicz,B.J. (1995) *NDR1*, a locus of *Arabidopsis thaliana* that is required for disease resistance to both a bacterial and a fungal pathogen. *Proc. Natl Acad. Sci. USA*, **92**, 6597–6601.

Century,K.S., Shapiro,A.D., Repetti,P.P., Dahlbeck,D., Holub,E. and Staskawicz,B.J. (1997) NDR1, a pathogen-induced component required for *Arabidopsis* disease resistance. *Science*, **278**, 1963–1965.

Connell,P., Ballinger,C.A., Jiang,J., Wu,Y., Thompson,L.J., Hohfeld,J. and Patterson,C. (2001) The co-chaperone CHIP regulates protein triage decisions mediated by heat-shock proteins. *Nat. Cell Biol.*, **3**, 93–96.

Dangl,J.L. and Jones,J.D.G. (2001) Plant pathogens and integrated defence responses to infection. *Nature*, **411**, 826–833.

Daniels,M.J., Mirkov,T.E. and Chrispeels,M.J. (1994) The plasma membrane of *Arabidopsis thaliana* contains a mercury-insensitive aquaporin that is a homolog of the tonoplast water channel protein TIP. *Plant Physiol.*, **106**, 1325–1333.

Dubacq,C., Guerois,R., Courbeyrette,R., Kitagawa,K. and Mann,C. (2002) Sgt1p contributes to cyclic AMP pathway activity and physically interacts with the adenylyl cyclase Cyr1p/Cdc35p in budding yeast. *Eukaryot. Cell*, **1**, 568–582.

Freeman,B.C. and Yamamoto,K.R. (2002) Disassembly of transcriptional regulatory complexes by molecular chaperones. *Science*, **296**, 2232–2235.

Garcia-Ranea,J.A., Mirey,G., Camonis,J. and Valencia,A. (2002) p23 and HSP20/α-crystallin proteins define a conserved sequence domain present in other eukaryotic protein families. *FEBS Lett.*, **529**, 162–167.

Grant,M.R., Godiard,L., Straube,E., Ashfield,T., Lewald,J., Sattler,A., Innes,R.W. and Dangl,J.L. (1995) Structure of the *Arabidopsis RPM1* gene enabling dual specificity disease resistance. *Science*, **269**, 843–846.

Hinsch,M. and Staskawicz,B.J. (1996) Identification of a new *Arabidopsis* disease resistance locus *RPS4* and cloning of the corresponding avirulence gene, *avrRps4*, from *Pseudomonas syringae* pv. *pisi. Mol. Plant-Microbe Interact.*, **9**, 55–61.

Holt,B.F., Hubert,D.A. and Dangl,J.L. (2003) Resistance gene signaling in plants—complex similarities to animal innate immunity. *Curr. Opin. Immunol.*, **15**, 20–25.

Holub,E.B., Beynon,J.L. and Crute,I.R. (1994) Phenotypic and genotypic characterization of interactions between isolates of *Peronospora parasitica* and accessions of *Arabidopsis thaliana. Mol. Plant-Microbe Interact.*, **7**, 223–239.

Hwang,C.F. and Williamson,V.M. (2003) Leucine-rich repeat-mediated intramolecular interactions in nematode recognition and cell death signaling by the tomato resistance protein Mi. *Plant J.*, **34**, 585–593.

Jander,G., Norris,S.R., Rounsley,S.D., Bush,D.F., Levin,I.M. and Last,R.L. (2002) *Arabidopsis* map-based cloning in the post-genome era. *Plant Physiol.*, **129**, 440–450.

Kaneko,T., Kotani,H., Nakamura,Y., Sato,S., Asamizu,E., Miyajima,N. and Tabata,S. (1998) Structural analysis of *Arabidopsis thaliana* chromosome 5. V. Sequence features of the regions of 1,381,565 bp covered by twenty one physically assigned P1 and TAC clones. *DNA Res.*, **5**, 131–145.

Kitigawa,K., Skowyra,D., Elledge,S.J., Harper,J.W. and Hieter,P. (1999) *SGT1* encodes an essential component of the yeast kinetochore assembly pathway and a novel subunit of the SCF ubiquitin complex. *Mol. Cell*, **4**, 21–33.

Krishna,P., Reddy,R.K., Sacco,M., Frappier,J.R. and Felsheim,R.F. (1997) Analysis of the native forms of the 90 kDa heat shock protein (hsp90) in plant cytosolic extracts. *Plant Mol. Biol.*, **33**, 457–466.

Lai,B.T., Chin,N.W., Stanek,A.E., Keh,W. and Lanks,K.W. (1984) Quantitation and intracellular localization of the 85K heat shock protein by using monoclonal and polyclonal antibodies. *Mol. Cell. Biol.*, **4**, 2802–2810.

Lange,C.A., Shen,T. and Horwitz,K.B. (2000) Phosphorylation of human progesterone receptors at serine-294 by mitogen-activated protein kinase signals their degradation by the 26S proteasome. *Proc. Natl Acad. Sci. USA*, **97**, 1032–1037.

Larkin,J.C., Walker,J.D., Bolognesi-Winfield,A.C., Gray,J.C. and Walker,A.R. (1999) Allele-specific interactions between ttg and gl1 during trichome development in *Arabidopsis thaliana*. *Genetics*, **151**, 1591–1604.

Lu,R. *et al*. (2003) High throughput virus-induced gene silencing implicates heat shock protein 90 in plant disease resistance. *EMBO J.*, **22**, 5690–5699.

Lyapina,S.A., Correll,C.C., Kipreos,E.T. and Deshaies,R.J. (1998) Human CUL1 forms an evolutionarily conserved ubiquitin ligase complex (SCF) with SKP1 and an F-box protein. *Proc. Natl Acad. Sci. USA*, **95**, 7451–7456.

Mackey,D., Holt,B.F.,III, Wiig,A. and Dangl,J.L. (2002) RIN4 interacts with *Pseudomonas syringae* type III effector molecules and is required for RPM1-mediated disease resistance in *Arabidopsis*. *Cell*, **108**, 743–754.

Mackey,D., Belkhadir,Y., Alonso,J.M., Ecker,J.R. and Dangl,J.L. (2003) *Arabidopsis* RIN4 is a target of the type III virulence effector AvrRpt2 and modulates RPS2-mediated resistance. *Cell*, **112**, 379–389.

Mindrinos,M., Katagiri,F., Yu,G.-L. and Ausubel,F.M. (1994) The *A.thaliana* disease resistance gene *RPS2* encodes a protein containing a nucleotide-binding site and leucine-rich repeats. *Cell*, **78**, 1089–1099.

Moffett,P., Farnham,G., Peart,J. and Baulcombe,D.C. (2002) Interaction between domains of a plant NBS-LRR protein in disease resistance-related cell death. *EMBO J.*, **21**, 4511–4519.

Muskett,P.J., Kahn,K., Austin,M.J., Moisan,L.J., Sadanandom,A., Shirasu,K., Jones,J.D.G. and Parker,J.E. (2002) *Arabidopsis RAR1* exerts rate-limiting control of *R* gene-mediated defence against multiple pathogens. *Plant Cell*, **14**, 979–992.

Nimchuk,Z., Marois,E., Kjemtrup,S., Leister,R.T., Katagiri,F. and Dangl,J.L. (2000) Eukaryotic fatty acylation drives plasma membrane targeting and enhances function of several type III effector proteins from *Pseudomonas syringae*. *Cell*, **101**, 353–363.

Obermann,W.M., Sondermann,H., Russo,A.A., Pavletich,N.P. and Hartl,F.U. (1998) *In vivo* function of Hsp90 is dependent on ATP binding and ATP hydrolysis. *J. Cell Biol.*, **143**, 901–910.

Panaretou,B., Prodromou,C., Roe,S.M., O'Brien,R., Ladbury,J.E., Piper,P.W. and Pearl,L.H. (1998) ATP binding and hydrolysis are essential to the function of the Hsp90 molecular chaperone *in vivo*. *EMBO J.*, **17**, 4829–4836.

Pratt,W.B. and Toft,D.O. (2003) Regulation of signaling protein function and trafficking by the hsp90/hsp70-based chaperone machinery. *Exp. Biol. Med.*, **228**, 111–133.

Prodromou,C., Roe,S.M., O'Brien,R., Ladbury,J.E., Piper,P.W. and Pearl,L.H. (1997) Identification and structural characterization of the ATP/ADP-binding site in the Hsp90 molecular chaperone. *Cell*, **90**, 65–75.

Queitsch,C., Sangster,T.A. and Lindquist,S. (2002) Hsp90 as a capacitor of phenotypic variation. *Nature*, **417**, 618–624.

Richter,K., Muschler,P., Hainzl,O. and Buchner,J. (2001) Coordinated ATP hydrolysis by the Hsp90 dimer. *J. Biol. Chem.*, **276**, 33689–33696.

Ritter,C. and Dangl,J.L. (1995) The *avrRpm1* gene of *Pseudomonas syringae* pv. *maculicola* is required for virulence on *Arabidopsis*. *Mol. Plant-Microbe Interact.*, **8**, 444–453.

Ritter,C. and Dangl,J.L. (1996) Interference between two specific pathogen recognition events mediated by distinct plant disease resistance genes. *Plant Cell*, **8**, 251–257.

Segnitz,B. and Gehring,U. (1997) The function of steroid hormone receptors is inhibited by the hsp90-specific compound geldanamycin. *J. Biol. Chem.*, **272**, 18694–18701.

Shirasu,K. and Schulze-Lefert,P. (2003) Complex formation, promiscuity and multi-functionality protein interactions in disease resistance pathways. *Trends Plant Sci.*, **8**, 252–258.

Takahashi,A., Casais,C., Ichimura,K. and Shirasu,K. (2003) HSP90 interacts with RAR1 and SGT1 and is essential for RPS2-mediated disease resistance in *Arabidopsis*. *Proc. Natl Acad. Sci. USA*, **100**, 11777–11782.

Tör,M., Gordon,P., Cuzick,A., Eulgem,T., Sinapidou,E., Mert,F., Can,C., Dangl,J.L. and Holub,E.B. (2002) *Arabidopsis* SGT1b is required for defense signaling conferred by several downy mildew (*Peronospora parasitica*) resistance genes. *Plant Cell*, **14**, 993–1003.

Tornero,P. and Dangl,J.L. (2001) A high throughput method for quantifying growth of phytopathogenic bacteria in *Arabidopsis thaliana*. *Plant J.*, **28**, 475–481.

Tornero,P., Chao,R., Luthin,W., Goff,S. and Dangl,J.L. (2002a) Large scale structure–function analysis of the *Arabidopsis RPM1* disease resistance protein. *Plant Cell*, **14**, 435–450.

Tornero,P., Merritt,P., Sadanandom,A., Shirasu,K., Innes,R.W. and Dangl,J.L. (2002b) *RAR1* and *NDR1* contribute quantitatively to disease resistance in *Arabidopsis* and their relative contributions are dependent on the *R* gene assayed. *Plant Cell*, **14**, 1005–1015.

Triantafilou,M., Miyake,K., Golenbock,D.T. and Triantafilou,K. (2002) Mediators of innate immune recognition of bacteria concentrate in lipid rafts and facilitate lipopolysaccharide-induced cell activation. *J. Cell Sci.*, **115**, 2603–2611.

Wallace,A.D. and Cidlowski,J.A. (2001) Proteasome-mediated glucocorticoid receptor degradation restricts transcriptional signaling by glucocorticoids. *J. Biol. Chem.*, **276**, 42714–42721.

Warren,R.F., Henk,A., Mowery,P., Holub,E. and Innes,R.W. (1998) A mutation within the leucine-rich repeat domain of the *Arabidopsis* disease resistance gene *RPS5* partially suppresses multiple bacterial and downy mildew resistance genes. *Plant Cell*, **10**, 1439–1452.

Warren,R.F., Merritt,P.M., Holub,E.B. and Innes,R.W. (1999) Identification of three putative signal transduction genes involved in R gene-specified disease resistance in *Arabidopsis*. *Genetics*, **152**, 401–412.

Whitesell,L. and Cook,P. (1996) Stable and specific binding of heat shock protein 90 by geldanamycin disrupts glucocorticoid receptor function in intact cells. *Mol. Endocrinol.*, **10**, 705–712.

Yabe,N., Takahashi,T. and Komeda,Y. (1994) Analysis of tissue-specific expression of *Arabidopsis thaliana* HSP90-family gene HSP81. *Plant Cell Physiol.*, **35**, 1207–1219.

Zhu,F.G. and Pisetsky,D.S. (2001) Role of the heat shock protein 90 in immune response stimulation by bacterial DNA and synthetic oligonucleotides. *Infect. Immun.*, **69**, 5546–5552.

Received July 7, 2003; revised September 2, 2003; accepted September 4, 2003

Supplementary Material

Supplementary Figure 1: *LRA2* is *HSP90.2*. (A) Map based cloning of *lra2* mutants began with genetic definition of a 52 kB interval on the lower arm of Chromosome V using the markers shown on the left and right. This region was contained on the P1 clone MDA7 (Kaneko et al., 1998). Candidate clones, including all three of the constitutively expressed cytosolic HSP90s in Arabidopsis, are given in green with the arrow pointing in the direction of transcription.

Supplementary Figure 2: Phenotypic pleiotropy in *hsp90.2* mutants suggests functions in additional Arabidopsis processes. While overall morphology is unaffected (row 1), *hsp90.*2 mutants show slight flattening of the leaves (adaxial view row 2 and abaxial view row 3), and young flower buds are not completely closed (row 4). Leaves often appeared somewhat flattened in *hsp90.2*. We often found that all the buds in a flower cluster were slightly opened prematurely. We did not observe a difference in gross morphological architecture of the roots. These phenotypes were weak and the bud phenotype was variably penetrant in all *hsp90.2* alleles, in contrast to the disease resistance phenotype. We recapitulated heat shock conditions known to cause loss of *R* function in other systems, notably the tobacco *N* gene, but failed to see an effect on *RPM1* function in wild type plants at 30°C. These same conditions also revealed no pronounced phenotypic effects in *hsp90.2* plants.

Supplementary Figure 3: SGT1a and Sgt1b contain strong structural similarity to two different HSP90 co-chaperones, HOP and p23. (A) The TPR motifs of AtSGT1s are predicted to fold like the TPR motif of the HSP90 co-chaperone, HOP (seen here).

(B) The CS domain found in AtSGT1s is predicted to fold in a similar conformation as p23 (seen here).

Sup. Fig. 1

A

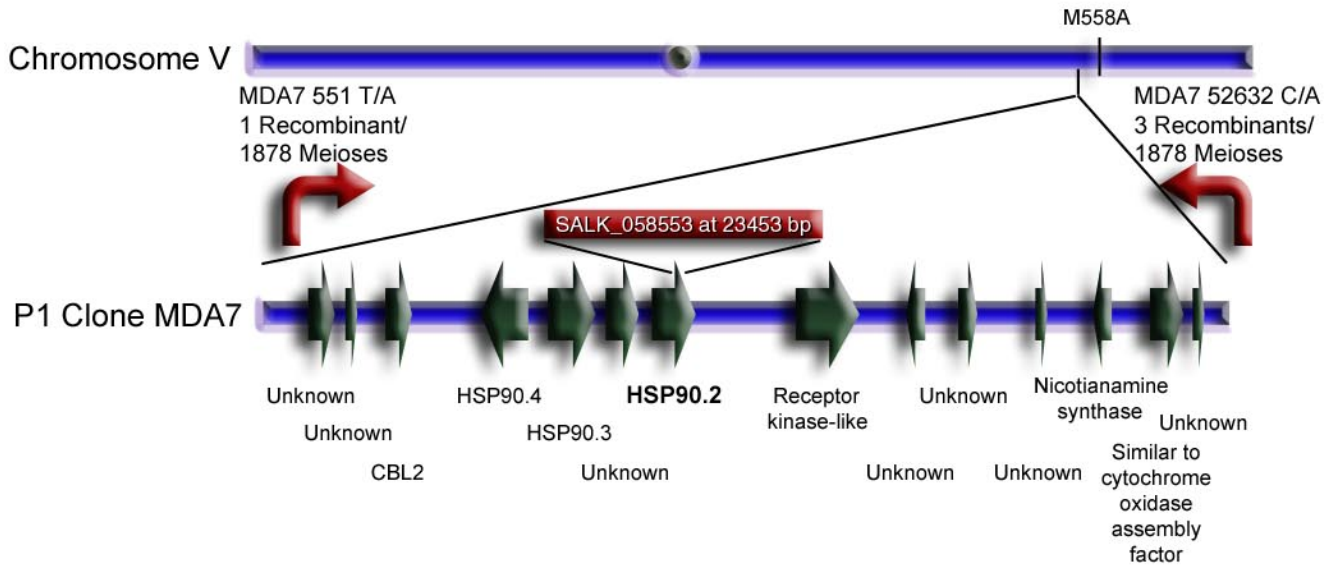
M558A
Chromosome V
MDA7 551 T/A
1 Recombinant/
1878 Meioses
MDA7 52632 C/A
3 Recombinants/
1878 Meioses
SALK_058553 at 23453 bp
P1 Clone MDA7
Unknown
Unknown
CBL2
HSP90.4
HSP90.3
Unknown
HSP90.2
Receptor
kinase-like
Unknown
Unknown
Unknown
Nicotianamine
synthase
Unknown
Similar to
cytochrome
oxidase
assembly
factor

Sup. Fig. 2

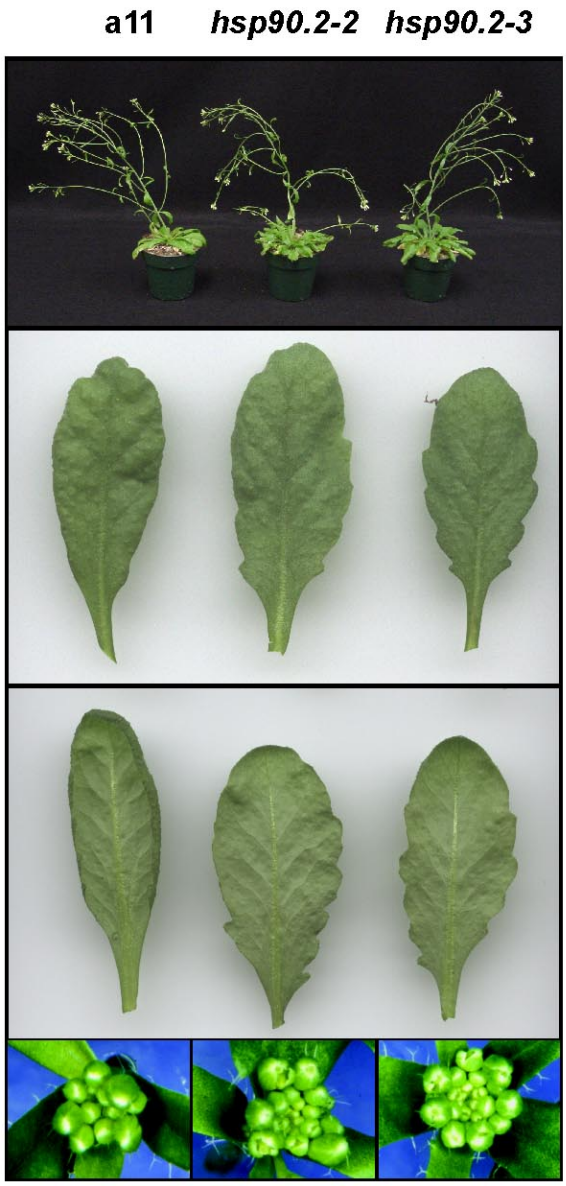

Sup. Fig. 3

A

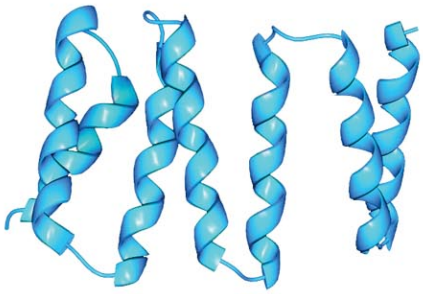

B